논문 2006-43TC-1-5

# 41° YX $LiNbO_3$ 기반 SAW 압력센서 개발

## ( Novel SAW-based pressure sensor on 41° YX-$LiNbO_3$ )

왕 웬*, 이 기 근**, 황 정 수*, 김 근 영*, 양 상 식**

( Wen Wang, Keekeun Lee, Jungsoo Hwang, Geunyoung Kim, and Sangsik Yang )

요 약

Single phase unidirectional transducer (SPUDT), 리플랙터, 웨이퍼 본딩 패키지로 구성된 표면탄성파 (surface acoustic wave, SAW) 기반 압력센서가 개발되어 졌다. Coupling of Mode (COM) 모델링에 의한 소자의 시뮬레이션 및 최적 설계 변수가 얻어졌다. Finite Element Methods (FEM)를 통해 주어진 압력에 따른 다이어프램 벤딩, 스트레인/스트레스 변화 및 SAW 속도변위가 미리 예측되어졌다. 유출된 최적 설계 변수를 이용 440 MHz SAW 기반 압력센서가 41o YX LiNbO3 기판 위에서 제작되어졌다. 고 S/N 비, 임펄스 리프렉션 피크, 작은 에러 피크가 관찰되어졌다. 측정된 S11 결과는 COM 모델링 및 FEM 시뮬레이션 결과와 일치함을 보였다.

Abstract

This paper presents a novel surface acoustic wave (SAW)-based pressure sensor, which is composed of single phase unidirectional transducer (SPUDT), three reflectors, and a deep etched substrate for bonding underneath the diaphragm. Using the coupling of modes (COM) theory, the SAW device was simulated, and the optimized design parameters were extracted. Finite Element Methods (FEM) was utilized to calculate the bending and stress/strain distribution on the diaphragm under a given pressure. Using extracted optimal design parameters, a 440 MHz reflective delay line on 41o YX LiNbO3 was developed. High S/N ratio, sharp reflection peaks, and small spurious peaks were observed. The measured S11 results showed a good agreement with simulated results obtained from coupling-of-modes (COM) modeling and Finite Element Method (FEM) analysis.

**Keywords**: Coupling of modes, Finite element method, Pressure sensor, SAW reflective delay line

## I. Introduction

Recently wireless and passive surface acoustic wave (SAW) based pressure sensor have gained increasing attraction in consumer electronics and communication systems, and some groups have reported successful application of the sensor[1][2]. However, the present SAW sensor suffers from large signal attenuation, broad reflection peaks, obvious noise and signal evaluation error. Until performance of the sensor do meet commercial requirements, the sensor will not be suitable for practical applications such as tire pressure monitoring system and human-recognizing sensor unit.

This paper presents a novel SAW-based pressure sensor on 41o YX LiNbO3, which is composed of a SAW reflective delay line with Single Phase Unidirectional Transducers (SPUDT) structure and a deep etched substrate underneath the diaphragm. Fig. 1(a) shows the schematic diagram of the sensor. A RF pulse is received by the contact pads of the SAW sensor. The inter-digital transducer (IDT), which is connected to the pads, transforms the received signal into a SAW. Reflectors are placed in the propagation path of the SAW at which small parts of the SAW

* 학생회원, ** 정회원, 아주대학교 전자공학부
(Div. of Electronics Engineering, Ajou University)
접수일자 : 2005년12월15일, 수정완료일 : 2005년1월19일

are reflected. The reflected waves are reconverted into an electromagnetic wave by the IDT and are transmitted to the measurement unit. A pressure difference induces the bending of the diaphragm. The bending changes SAW propagation length and velocity, resulting in the phase shifts of the reflected peaks depending on applied pressure values. By evaluating the phase shifts, we can extract external pressure values. Fig. 1(b) shows simple schematic diagram of the SPUDT structure used for the device. The basic idea of SPUDT is to enhance the generated signal in the forward direction but reduce the signal in the reverse direction using the distributed reflection sources in the inter-digital transducer[3].

Using the coupling of modes (COM) theory[4], the SAW reflective delay line with three reflectors and SPUDT structure was simulated. The optimal design parameters were extracted. Using the Finite Element Method (FEM) program, the stress/strain distribution and velocity shift on the diaphragm under a given pressure was calculated, and the configuration of the sensor was determined. This paper presents methods to simulate the devices, the process used to create reliable SAW sensor, electrical and mechanical performances, and comparison between simulated and measured results.

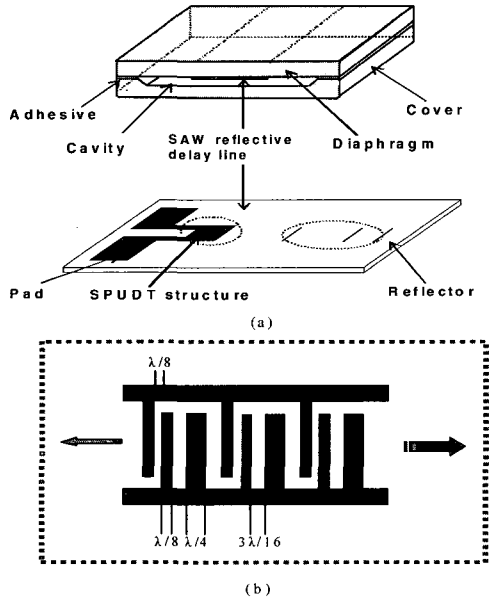


그림 1 .(a) 제작될 SAW 압력센서, (b) SPUDT 구조
Fig. 1. (a) Schematic diagram of the SAW-based pressure sensor and (b) magnified view of the SPUDT structure.

## II. Analysis model and computer simulation

### 1. Coupling-of-modes (COM) mode

COM is a computationally very efficient technique developed for the analysis of the SAW device in which small distributed internal reflections are important, such as SPUDT structure. It is an elegant method for modeling systems with spatially or time varying properties. In 1976 and 1977 Suzuki et al.[5] and Haus[6][7] introduced the COM theory in the SAW field. The COM equation for the SAW device with SPUDT was deduced by Write[4] as described in eq. (1), which were written in terms of the mode's slowly varying amplitudes, while the equations presented here are written directly in terms of $R(x)$ and $S(x)$ shown in Fig. 2.

$$\begin{cases} \dfrac{dR(x)}{dx} = -jk_E R(x) + j\kappa_R e^{-j2k_0 x} S(x) + j\alpha_R(x) e^{-jk_0 x} V_T \\ \dfrac{dS(x)}{dx} = jk_E S(x) - j\kappa_s e^{j2k_0 x} R(x) - j\alpha_s(x) e^{jk_0 x} V_T \\ \dfrac{dI(x)}{dx} = -j\omega C(x) V_T + j2\alpha(x) e^{jk_0 x} R(x) + j2\alpha(x) e^{-jk_0 x} S(x) \end{cases} \quad (1)$$

where

$$k_E = \frac{\omega}{v_R} \frac{8\alpha^2 \omega C_T R_E^2 \Lambda_T}{1+(2\omega C_T R_E)^2} - j\left(\gamma + \frac{4\alpha R_E \Lambda_T}{1+(2\omega C_T R_E)^2}\right)$$

$$k_0 = \frac{2\pi}{\Lambda_T} \qquad \alpha_R = \frac{\alpha e^{+j\Phi_k}}{1+2j\omega C_T R_E}$$

$$\alpha_s = \alpha_R^* = \frac{\alpha e^{-j\Phi_k}}{1+2j\omega C_T R_E}$$

$$\kappa_R = \kappa e^{-j\Phi_k} + \frac{4jR_E \Lambda_T \alpha^2 e^{+2j\Phi_a}}{1+2j\omega C_T R_E}$$

$$\kappa_s = \kappa e^{+j\Phi_k} + \frac{4jR_E \Lambda_T \alpha^2 e^{-2j\Phi_a}}{1+2j\omega C_T R_E}$$

Here $L$ the length of the section, $\Lambda_T$ the wavelength of transduction, $k_0$ the wavenumber, $k$ the reflectivity per unit length, $\alpha$ the transduction strength per unit length, $\Phi_a$ the phase of transduction, $\Phi_k$ the phase of reflection, $C_T$ interdigital capacitance

in one transduction period, $\Upsilon$ the propagation low per unit length, $R_E$ the effective thin film resistance in one transduction period, $v_R$ the SAW velocity, and $\omega$ the angle frequency.

The mixed (P) matrix representation[8][9] was used to present the solutions to the COM equations. In the P matrix representation the acoustic ports are treated as scattering ports, while the electric port is treated as an admittance port.

$$\begin{bmatrix} S(0) \\ R(L) \\ I(0) \end{bmatrix} = \begin{bmatrix} P_{11} & P_{12} & P_{13} \\ P_{21} & P_{22} & P_{23} \\ P_{31} & P_{32} & P_{33} \end{bmatrix} \begin{bmatrix} R(0) \\ S(L) \\ V_0 \end{bmatrix} \tag{2}$$

The mixed matrix solutions for a uniform transducer section were derived from the integral solutions. Based on the cascading relationships[10], the resultant $P$ matrices are cascaded for the complete transducer represented as $P_{IDT}$. And the $P$ matrices for the reflectors can also be cascaded as $P_{ref}$. The admittance matrix for the device can be derived according to

$$Y = \begin{bmatrix} y_{11} & y_{12} \\ y_{21} & y_{22} \end{bmatrix} \tag{3}$$

where

$$y_{11} = P_{IDT33} + \frac{P_{ref11} P_{IDT32} P_{IDT23}}{1 - P_{ref11} P_{IDT22}}$$

$$y_{12} = \frac{P_{ref13} P_{IDT32}}{1 - P_{ref11} P_{IDT22}}$$

$$y_{21} = \frac{P_{ref31} P_{IDT23}}{1 - P_{ref11} P_{IDT22}}$$

$$y_{22} = P_{ref33} + \frac{P_{IDT22} P_{ref13} P_{ref31}}{1 - P_{ref11} P_{IDT22}}$$

Then, the reflection coefficient $S_{11}$ can be deduced by

$$S_{11} = \frac{(Y_G - y_{11}) \times (Y_G + y_{22}) + y_{12} \times y_{21}}{(Y_G + y_{11}) \times (Y_G + y_{22}) - y_{12} \times y_{21}} \tag{4}$$

Here, $Y_G$ is the resource and load inductance.

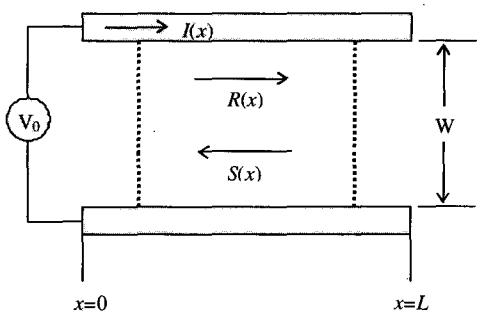


그림 2. COM 모델링을 위한 소자 변수들
Fig. 2. SAW schematic and variables for COM theory.

## 2. COM simulation

The 440 MHz SAW reflective delay line with three reflectors and SPUDT structure is simulated (reflection coefficient $S_{11}$ in time domain) based on the COM theory explained above and the results are summarized in the following section. The optimal design parameters were also determined. The design parameters used for the simulation were shown in the Table 1. A 41° YX $LiNbO_3$ piezoelectric substrate was used because of its high SAW propagation velocity (4750 m/s) and large values of electromechanical coupling factors $K^2$ (15.8%)[11].

Table 1 shows the effect of number of IDT finger pairs and acoustic aperture on the device characteristics. $\lambda$ is the wavelength corresponding to the operation frequency. Group 1 shows two reflective delay lines with different number of IDT pairs. Decrease in the number of IDT can lower the loss of the device and improve the S/N ratio. Group 2 shows two reflective delay lines with different aperture. The acoustic aperture only affects the dynamic separation within the time response. With the increasing of acoustic aperture, the dynamic separation is decreased.

Fig. 3 shows two different curves for reflective delay line with different type reflector. It can be seen that the loss becomes smaller by using the IDT finger pair as the reflector than the Bar type reflector. However, because of the self-reflection in the IDT type reflector, there are more small peaks occurred between the reflector peaks in time domain.

As a summary from the simulated results, decrease of the IDT pair number, selection of apt acoustic

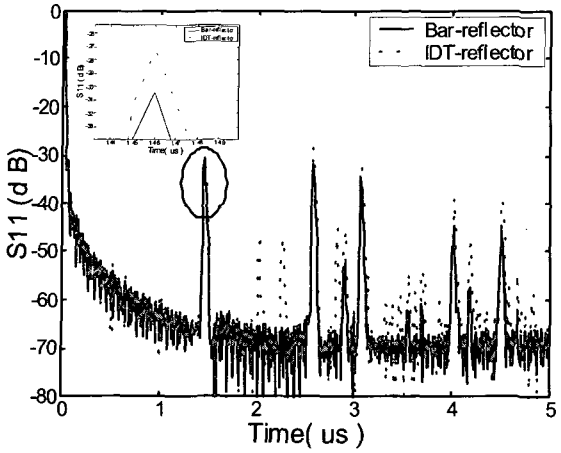


그림 3. 두 다른 리프렉터 타입에 따른 S11 시뮬레이션 결과

Fig. 3. Simulated S11 values in time domain of 440 MHz reflective delay line with two different type reflector, bar and IDT.

표 1. 제작된 SAW 압력센서의 설계 변수 효과

Table 1. The effect of structure parameters on the SAW device characteristics.

| | | Group.1 | | Group.2 | |
|---|---|---|---|---|---|
| Device Parameters | IDT pair number | 10 | 50 | 10 | 10 |
| | Aperture | 50λ | 50 λ | 50 λ | 100 λ |
| | Reflector type | Bar | Bar | Bar | Bar |
| | Electrode material | Al | Al | Al | Al |
| Properties for 1st reflector peak | Loss (dB) | 35 | 44 | 35 | 34 |
| | Bandwidth/70dB (μs) | 0.09 | 0.16 | 0.089 | 0.083 |
| | Dynamic separation (dB) | 80 | 78 | 80 | 70 |

aperture, and using of bar reflector should be good choices to improve the performance of the sensor.

## 3. FEM analysis

To determine the sensor configuration, it is necessary to calculate the diaphragm bending and stress/strain distribution on the diaphragm. Because it is difficult to compute the mechanics of anisotropic material analytically, a Finite Element Method (FEM) and software ANSYS is used to analysis the diaphragm under applied mechanical force. Because the diaphragm thickness is much less than its size usually, the diaphragm can regarded as a shell. The dimension of the diaphragm is assumed to 5mm ×3mm×350μm, and it is divided as finite small units with four nodes. Under a fixed boundary situation and certain pressure, the stress and strain distribution on the diaphragm can calculated using FEM program, ANSYS software.

Fig. 4 shows calculated bending of the $LiNbO_3$ diaphragm at a pressure of 300 kPa by ANSYS software. Fig. 5 shows the X-direction strain distribution of the SAW guiding layer of the diaphragm at a pressure of 300 kPa. Results show that there exist compressed and stretched sections along the bended diaphragm. According to the analysis method of Taziev[12], the acoustic velocity shift can also be calculated, as shown in Fig. 5. From the figure, it is known that the SAW propagation velocity is slower in the stretched section, whereas it is faster in the compressed section. Stretched section is observed near the center of the diaphragm, while compressed strain section was observed near the edge

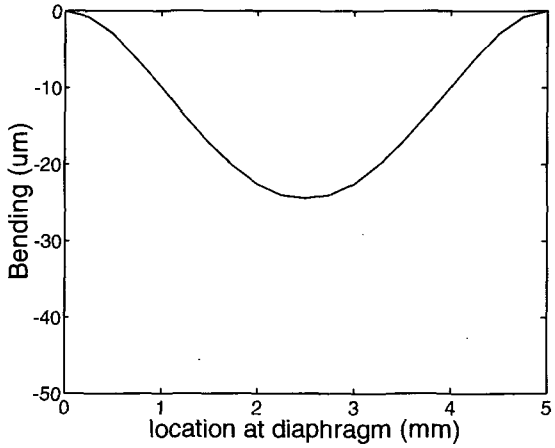


그림 4. 300 kPa 압력하에 ANSYS를 이용 계산되어진 다이어프램 휨 정도

Fig. 4. Calculated bending of the diaphragm at a 300 kPa pressure based on ANSYS software.

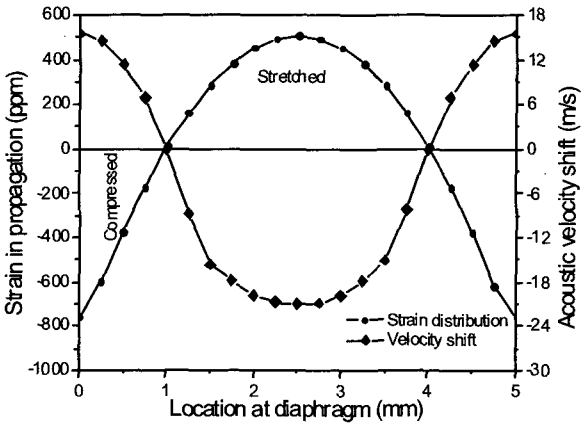


그림 5. 300 kPa 압력에 x 방향으로의 다이어프램 스트레인 및 속도 변화

Fig. 5. Calculated X direction strain of the diaphragm and velocity shift at a 300 kPa pressure.

of the diaphragm. observed near the edge of the diaphragm. As a SAW pressure sensor with three reflectors, to avoid large temperature sensitivity, the first and second reflectors are placed at a stretched position, and the third reflector is placed at a compressed position, the border of the diaphragm.

## III. Fabrication

According to the simulated result as above, a new 440MHz SAW reflective delay line with three reflectors was developed. The design parameters are shown in Table 2. Three reflectors were arranged along the SAW propagation direction. Based on the FEM analysis, the configuration of the device was determined, the center to center distance between the IDT and 1st reflector is about 2980 μm, the center to center distance between the 2nd and 1st reflector is about 1124 μm, and the center to center distance between the 2nd and 3rd reflector is about 250 μm.

The schematic diagram for fabrication procedure is shown in Fig. 6. A 4″ 41° YX $LiNbO_3$ piezoelectric substrate with 350 μm thickness was used because of its high SAW velocity and large electromechanical coupling factor $K^2$. Wafer was cleaned at acetone and rinsed in DI water. A 1 μm thick photoresist (PR) was spin-coated, exposed, and then patterned for IDT and three reflectors. Reactive ionic etching (RIE) was used to etch away the PR residue on the patterned piezoelectric substrate. A 1500Å thick aluminum was deposited for IDT and three reflectors on piezoelectric substrate using electron beam evaporator.

After aluminum evaporation, the PR was dissolved in acetone for 2 hrs for lift-off processing. Several rinses with de-ionized water were performed to remove any unwanted products. The substrate was dicing-sawed for wafer bonding and package. To bend the diaphragm during pressure, a 200μm deep cavity on heavily doped silicon substrate was made in Tetramethyl Ammonium Hydroxide (TMAH) solution using $SiO_2$ masking layer. Heavily doped Si substrate provides low resistivity like metal, resulting in good ground shielding during network analyzer measurement. Gold was deposited over bottom substrate using sputter for ground shielding. The diaphragm was then attached to the silicon substrate with an epoxy adhesive.

The fabricated device with SPUDT structure was

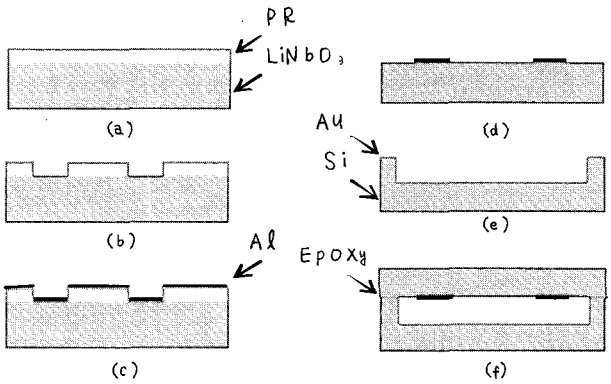


그림 6. SAW 압력센서 제작 과정: (a) PR 코팅, (b) PR 패턴닝, (c) 알루미늄 증착, (d) 리프트 오프, (e) 실리콘 에칭 및 그라운드 쉴딩, (f) 에폭시를 이용 웨이퍼 본딩

Fig. 6. Fabrication procedure of the SAW pressure sensor: (a) PR spinning, (b) PR patterning for an IDT and three reflectors, (c) aluminum deposition, (d) lift-off, (e) heavily doped silicon etching and ground shielding with gold, and (f) wafer bonding with epoxy.

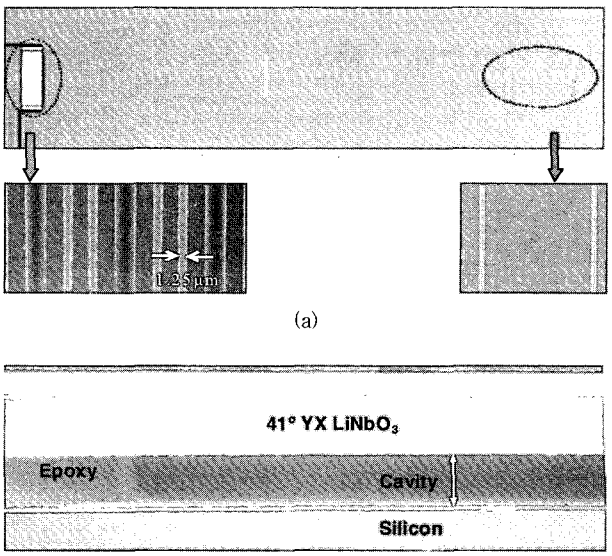


그림 7. 제작되어진 SAW 센서 광학 사진 및 SEM 사진. (a) 전체 사진, (b) 완성된 웨이퍼 본딩

Fig. 7. Optical microscope and SEM pictures of the fabricated SAW pressure sensor with SPUDT structure. (a) Total top view, (b) wafer bonding between the diaphragm and ground-shielded silicon with epoxy.

표 2. 제작된 SAW 센서 설계 파라미터들
Table 2. Design parameters of the fabricated SAW-based pressure sensor.

| | Design parameters | | Design parameters |
|---|---|---|---|
| Cent frequency | 440MHz | Acoustic aperture | 50λ |
| IDT pair number | 20 | Electrode material | Al |
| Reflector number | 3 | Diaphragm dimension (Length, Width, Thickness) | (5mm,3mm,350μm) |
| Reflector type | Bar | Substrate material | 41°YX-$LiNbO_3$ |

visualized through optical microscope and scanning electron microscopy (SEM), as shown in Fig. 7. The smallest IDT finger width was 1.25μm, aluminum thickness was 0.1μm, and overlapping aperature was 200μm. Three reflectors were arranged in a row. The ratio of the distance between the first reflector and second to the distance between the second and third which is denoted as weighting factor[13] was 5 to minimize temperature dependence effect. The diaphragm was attached to the bottom silicon substrate with a 200μm deep cavity using an epoxy adhesive, as shown in Fig. 7(b).

## IV. Experimental results and discussion

The reflection coefficient $S_{11}$ in time domain of the SAW device was measured using HP 8510 network analyzer and Cascade probe station, as shown in Fig. 8 (the solid line). Three clear peaks were observed from three reflectors. Large S/N ratio, sharp peaks, and high dynamic separation between the peaks were observed. The first reflection occurred at 1.3μs, and at that point $S_{11}$ was ~35dB. The measured result shows a good agreement with simulated one (the dotted line in Fig. 8). The rest of small peaks are considered from multiple reflections between the periodically spaced reflectors and edge reflections.

Next a mechanical pressure was applied from 0kPa to 400kPa on the diaphragm of sensor, and Fig. 9 shows the sensitivity evaluation of the sensor, and there is a good linearity between the phase shifts and pressure in the pressure of 0kPa to 300kPa. The sensitivity was evaluated as about 2.6/kPa.

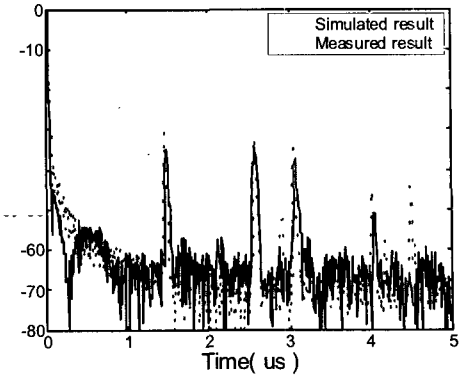


그림 8. 무압력상태에서 S11 시뮬레이션 및 측정 결과들
Fig. 8. Simulated and Measured S11 values in time domain in case of no pressure.

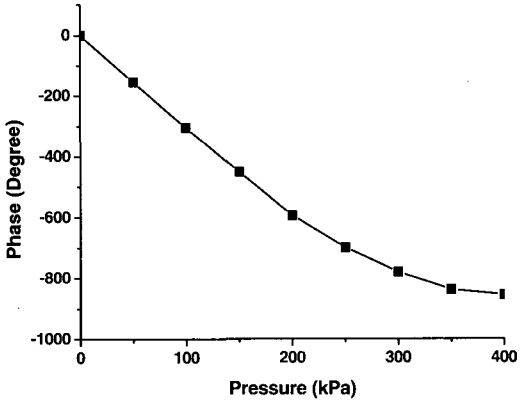


그림 9. 압력에 따른 페이즈 변위
Fig. 9. Phase shifts versus pressure for SAW-based pressure sensor.

## V. Conclusion

A novel SAW pressure sensor composed of a reflective delay line with SPUDT structure and a bond substrate underneath the diaphragm was developed. Using COM theory, SAW device was simulated, and the optimal design parameters were also determined. It was observed that decreasing of number of IDT finger pairs can lower the loss of the device and improve the S/N ratio. The acoustic aperture affects the dynamic separation between the reflection peaks within the time response. Selection of the bar reflector can improve the performance of the device obviously. In order to determine the configuration of the device, Finite Element Method (FEM) was used to calculate the bending of the diaphragm and stress/strain distribution on diaphragm.

According to the simulated results and FEM analysis, a new 440 MHz reflective delay line on 41 YX $LiNbO_3$ was developed. A good agreement exists between the simulated and measured reflection coefficient $S_{11}$, high S/N ratio, sharp reflection peaks and high dynamic separation between the peaks were observed. The new SAW device was successfully applied for pressure sensor, and extracted sensitivity was approximately 2.6/kPa.

## Acknowledgments

The authors wish to acknowledge the support of the Ubiquitous Frontier 21 program under Ministry of Information and Communication Republic of Korea.

## 참 고 문 헌

[1] L. Reindl, A. Pohl, G. Scholl, and R. Weigel, "SAW based radio sensor systems", *IEEE Sensors Journal*, Vol. 1, No. 1, p. 69, 2001.

[2] G. Scholl, F. Schmidt, T. Ostertag, L. Reindl, H. Scherr, and U. Wolff, "Wireless passive SAW sensor systems for industrial and domestic applications", *IEEE Ultrasonics Symposium*, p. 595, 1998.

[3] C. S. Hartmann, P. V. Write, "Overview of Design Challenges for Single Phase Unidirectional SAW Filters", *IEEE Ultrasonic Symp.*, p. 79, 1989.

[4] P. V. Wright, "Analysis and design of Low-Loss SAW devices with internal reflections unsing Coupling-of-modes theory", *IEEE Ultrasonic Symp.*, p. 141, 1989.

[5] Y. Suzuki, H. Shimizu, M. Takeuchi, "Some studies on SAW resonators and multiple-mode filters", *IEEE Ultrasonics Symposium*, p. 297, 1976.

[6] H.A.Haus, "Modes in SAW grating Resonators", Journal of Applied physics, Vol. 48, No. 12, p. 4955, 1977.

[7] H. A. Haus, "Bulk Scattering loss of SAW grating cascades", *IEEE Transactions on Sonics and Ultrasonics*, Vol. 24, No. 4, p. 259, 1977.

[8] C. S. Hartmann and B. P. Abbott, "Generalized Impulse response Model for SAW Transducers including effects of Electrode reflections", *IEEE Ultrasonics symposium*, p. 29, 1988.

[9] G. Tobolka, "Mixed Matrix representation of SAW tranducers", *IEEE Transactions on Sonics and Ultrasonics*, Su-26, p. 426, 1979.

[10] B. P. Abbott, C. S. Hartmann, and D. C. Malocha, "A coupling of modes analysis of chirped transducers containing reflective electrode geometries", *IEEE Ultrasonics Symposium*, p. 129, 1989.

[11] K. Yamanouchi, K. Shibayama, "Propagation and Amplification of Rayleigh Waves and Piezoelectric leaky surface waves in LiNbO3", *J. App. Phys.*, Vol. 43, p. 856, 1972.

[12] R. M. Taziev, E. A. Kolosovsky, and A. S. Kpzlov, "Deformation-sensitive cuts for surface acoustic waves in α-quartz", *IEEE Frequency Control Symposium*, p. 660, 1993.

[13] H. Scherr, G. Scholl, F. Seifert, and R. Weigel, Quartz pressure sensor based on SAW reflective delay line", *IEEE Ultrasonics Symposium*, p. 347, 1996.

## 저 자 소 개


Wang, Wen
B.S. Central South University, Electrical Eng., 1999.
M.S. Central South University, Electrical Eng., 2001.
Ph. D. Institute of Acoustics, The Chinese Academy of Science, 2005.
Current Ajou University, Electronics Eng., Post doctor.
<Research Interests : SAW sensor, Modeling and Simulation>

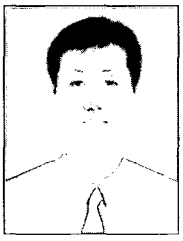

이 기 근 (정회원)
1988년 광운대학교 전자 학사
1993년 University of Florida 재료 석사
2001년 Arizona State University 전자 박사
현재 아주대학교 전자공학부 조교수
<주관심분야 : SAW 센서, Neural probes, RF MEMS>

황 정 수 (학생회원)
2004년 아주대학교 전자공학부 학사
현재 동 대학원 석사 과정
<주관심분야 : 센서, 디스플레이>

김 근 영 (학생회원)
1999년 아주대학교 전자공학부 학사
2002년 아주대학교 전자공학과 석사
현재 동 대학원 박사 과정
<주관심분야 : 초소형 구동기, 센서>

양 상 식 (정회원)
1980년 서울대학교 기계공학과 학사
1983년 서울대학교 기계공학과 석사
1988년 University of California at Berkeley 기계공학과 박사
현재 아주대학교 전자공학부 교수
<주관심분야 : 마이크로 소자의 Mechanism과 Actuation, Motion Control>